Unique growth mode observed in a Pb thin film on the threefold surface of an i-Ag-In-Yb quasicrystal

Sam Coates ⓘ, Stuart Thorn, Ronan McGrath ⓘ, and Hem Raj Sharma ⓘ

Surface Science Research Centre and Department of Physics, University of Liverpool, Liverpool L69 3BX, United Kingdom

An Pang Tsai

Institute of Multidisciplinary Research for Advanced Materials, Tohoku University, 2-1-1 Katahira, Aoba-ku, Sendai 980–8577, Japan

Novel epitaxial quasicrystalline films can be grown using the surfaces of intermetallic quasicrystals as templates. Here, we present a study of Pb adsorption on the threefold i-Ag-In-Yb surface, where Pb grows in a manner contrasting with conventional thin-film growth modes. Pb atoms are found to adsorb at sites over a range of heights, which are explained by bulk atomic positions left vacant by surface truncation, producing three-dimensional, isolated quasicrystalline Pb structures. This finding is contrasted with the growth of Pb on the more commonly used fivefold surface of the same quasicrystal, where smooth epitaxial layers result. We suggest that this unique structure originates due to the lower atomic density of the threefold surface, compared to the fivefold surface. Similar atomic density can be found in lower symmetry planes of periodic systems, but these planes are often unstable and become facetted. This stable low-density quasicrystalline substrate provides a facile route to achieve this type of templated growth.

I. INTRODUCTION

Quasicrystals are materials which exhibit long-range order yet are aperiodic [1]. As a result, they can exhibit intriguing geometric arrangements with unusual rotational symmetries which can be mapped using aperiodic tilings (e.g., the Penrose tiling [2]). In previous work, the surfaces of intermetallic quasicrystals have been utilized to produce epitaxial networks with exotic structures, where atoms and molecules occupy specific adsorption sites, creating highly ordered single-constituent quasicrystalline structures which have been "templated" by the surface structure [3–15].

A notable example is the deposition of Pb onto the fivefold surface of the icosahedral (i)-Ag-In-Yb quasicrystal, which possesses two-, three-, and fivefold symmetry axes. The bulk structure of i-Ag-In-Yb is modeled using i-Cd-Yb Tsai-type clusters, a hierarchical system of polyhedral "shells" which are decorated with either Cd or Yb (with Ag/In replacing Cd equally) [16]. Figure 1(a) shows the polyhedra (tetrahedron, dodecahedron, icosahedron, icosidodecahedron, and rhombic triacontahedron), which we will refer to as the first through fifth shells, respectively. These clusters are distributed aperiodically throughout the bulk with orientations defined by the high-symmetry directions. They are joined by "glue" units: interstitial polyhedra which are separate from the Tsai-type cluster [16].

When Pb is deposited onto the fivefold i-Ag-In-Yb surface, it is found to grow in a quasicrystalline layer-by-layer fashion, with the adsorption sites of each layer mirroring the structure of specific planes of atoms from the bulk model [17]. Figure 1(b) illustrates this. Here, a truncated Tsai-type cluster

is shown with the fourth shell in blue. The cluster center is marked with a golden atom. A horizontal arrow indicates the truncation, i.e., the surface. Shown above this truncation are positions of atoms of the fourth shell (shown as hollow circles) if cluster growth were to be continued above the surface. At the fivefold i-Ag-In-Yb surface, Pb is found to sit at certain positions and heights which can be explained by occupation of such bulklike planes [17]. The same has been found to be true for other elements, for example, Bi [18].

In this work, we show that this type of adsorption behavior is not specific to the fivefold termination of the i-Ag-In-Yb system. By dosing Pb onto the threefold i-Ag-In-Yb surface we observe the same general growth method; however, the resultant structure is different in nature. Here, instead of a layer-by-layer system, we observe isolated Pb structures which grow perpendicular to the surface. We link this behavior to the relative change in density of available adsorption sites between the threefold and fivefold surfaces.

II. METHODS

The threefold surface of an i-Ag-In-Yb quasicrystal was polished with successively finer grades of diamond paste (6–0.25 μm) before washing in methanol. After insertion into an ultrahigh-vacuum chamber, the surface was cleaned with sputter-anneal cycles (30 min Ar$^+$ sputter, 2 h anneal at 700 K). Substrate cleanliness was monitored with low-energy electron diffraction and scanning tunneling microscopy (STM). Pb was evaporated at a constant flux of 120 nA onto the surface using a Focus EFM 3 evaporator.
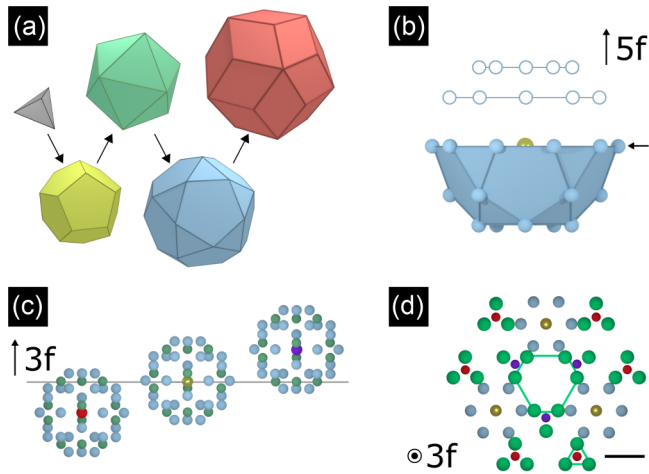
FIG. 1. (a) The hierarchical i-Cd-Yb cluster model. A Cd tetrahedron (gray), Cd dodecahedron (yellow), Yb icosahedron (green), Cd icosidodecahedron (blue), and Cd rhombic triacontahedron (red) are arranged concentrically to form the Tsai-type cluster. Arrows indicate hierarchy. (b) Side view of the fourth shell of a truncated cluster, oriented along its fivefold direction. The fivefold surface is marked with an arrow. The cluster center is shown as a golden atom. Also shown are planes of atoms from the fourth shell if the structure were continued "above" the surface. (c) Side view of how truncated clusters contribute to the threefold surface. Horizontal scale is arbitrary. (d) Arrangement of truncated bulk clusters as observed on the surface. A distorted hexagon and a triangle are marked to compare to STM images. The scale bar is 1 nm.

III. RESULTS

The clean threefold surface of the i-Ag-In-Yb quasicrystal was previously explored by STM [19]. When observed with nonatomic resolution, the surface appears to be populated by protrusions which form a quasicrystalline network of bright flowerlike triangles and so-called distorted hexagons. Atomic resolution is achieved through positive bias (reported as less than $+1.5$ V), where these larger protrusions are revealed to consist of sets of individual atoms. Figure 2(a) shows an example of the previously identified flower/distorted hexagon structure, with both motifs labeled. Vacancies are also highlighted by white circles. Figure 1(d) shows the equivalent structure in the model, with a distorted hexagon (marked in green) formed by Yb atoms. A small triangle is also highlighted, which forms one of the vertices of the flower motifs. In both nonatomic and atomic resolution cases, only Yb atoms are observed [19].

Due to the low atomic density of the surface and Yb atom bias, the substrate appears rough using STM, so that clearly resolving Pb atoms and their subsequent adsorption sites is difficult at low to medium coverages. The approach we take is to deposit Pb for a length of time similar to that used to obtain submonolayer coverage on the fivefold surface [17]. Then, assuming that the threefold surface has a sticking coefficient similar to that of the fivefold surface, we can compare the height and morphology of the Pb-dosed surface to the clean threefold surface.

Figure 2(b) shows an STM image of the surface after depositing Pb for 10 min, which would produce an approximate

coverage of ∼0.5 monolayer on the fivefold surface. Here, Pb protrusions form a morphologically rough quasicrystalline network, with many triangular features observed. The size of the individual spots which build the vertices of the triangular features suggests that multiple Pb atoms are contributing to each protrusion: Figs. 2(a) and 2(b) are the same scale, yet the protrusions in Fig. 2(b) appear larger than those in Fig. 2(a). Two triangular Pb motifs, labeled 1 and 2, are highlighted in Fig. 2(b), and the edge lengths are noted in Table I. Motifs rotated by $60°$ which share these edge lengths are marked by dotted lines. The quasicrystalline ordering of the Pb is evidenced by the inset fast Fourier transform (FFT), which was taken after isolating the Pb atoms in the image (i.e., filtering out the substrate contribution). High-intensity spots are scaled by τ, a hallmark of aperiodic order in quasicrystals.

To clearly distinguish the Pb atoms from the rough substrate, height histograms have been calculated from both Figs. 2(a) and 2(b). Figure 2(c) shows the histogram taken from the substrate. The main peak is broad, a reflection of the surface roughness, with the presence of vacancy defects and partial fragments of an incomplete terrace. The main peak also shows a slight asymmetry towards higher z values, which is indicative of the "flower" arrangements occasionally appearing brighter. Figure 2(d) shows the histogram from the Pb-dosed surface in Fig. 2(b). It has a different distribution from that of the substrate histogram, with a sharp peak bearing a shoulder to its left, at lower z. We attribute the higher peak to the Pb atoms, with the shoulder on the left originating from the surface. The small number of counts at higher z values are due to the growth of Pb atoms at a second height, which will be discussed later.

To highlight the difference between the two histograms, a composite is shown in Fig. 2(e). As the separate histograms show the absolute distribution of heights within each image—the definition of $z = 0$ is dependent on the individual scan—this composite has been shifted so that the substrate peaks overlap, and it has been scaled to allow for a direct comparison. The difference in shape and heights between the two plots clearly differentiates the Pb signal from the substrate.

Figures 3(a)–3(c) show the substrate after increasing Pb deposition time (15–120 min). As the dose time progresses, Pb atoms form a porous, quasicrystalline network of isolated triangular structures at four distinct heights. The quasicrystallinity of the Pb overlayer is shown by an FFT inset in Fig. 3(c), considering only atoms at the fourth height. Various motifs are numbered and labeled, and the edge lengths are noted in Table I.

Histograms taken from Figs. 3(a) and 3(c) are shown in Figs. 3(d) and 3(e), respectively. The evolution of the height distribution with respect to coverage can be seen in Fig. 3(d). As the surface becomes gradually covered with Pb, the prominence of the substrate shoulder signal is diminished, as the height 2 peak increases in size and sharpness. Large vacancies in the substrate are still observed by STM, however, as is apparent from the tail at low z. Figure 3(e) shows the Pb heights at the maximum observed coverage. Here, three peaks are discernible, with the substrate now completely covered by the first height of Pb, evident by the disappearance of the vacancy "tail" at low z. The prominence of the height 2 peak is also reduced, which indicates that Pb at height 3 or 4 (or
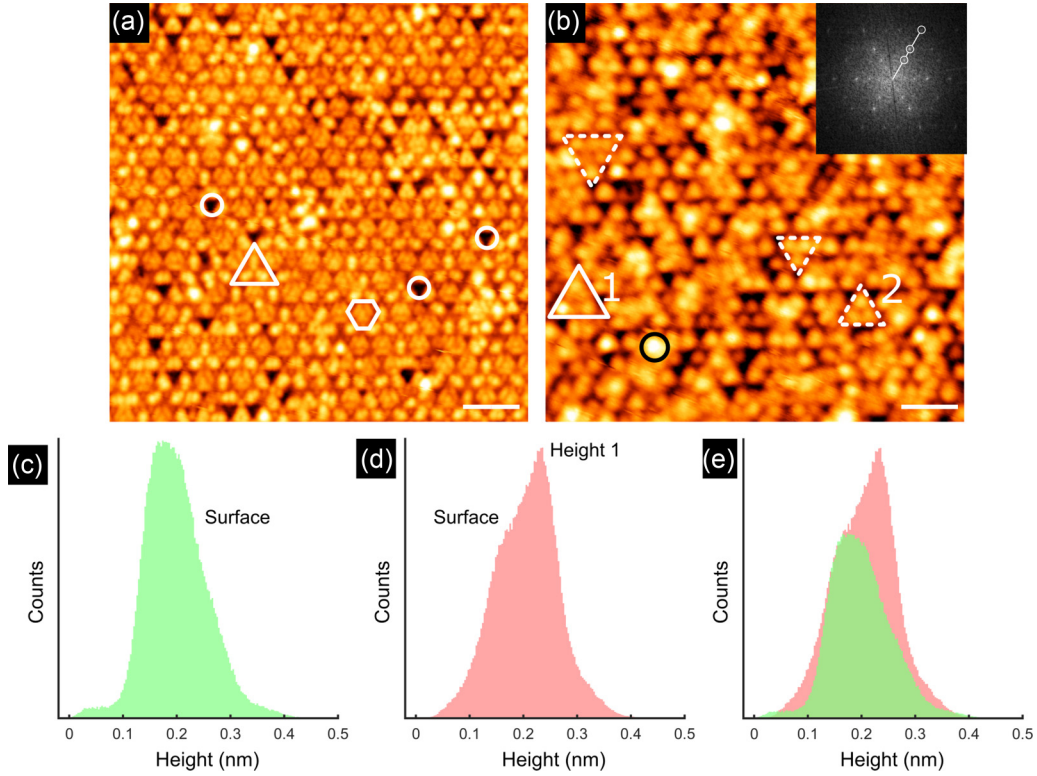
FIG. 2. (a) STM image of the clean substrate. The scale bar is 6 nm. Highlighted in white are triangles and distorted hexagons. (b) STM image of the surface after Pb dosing for 10 min. The scale bar is 6 nm. Highlighted in white and numbered 1 and 2 are two triangular motifs of different edge lengths. The dashed triangles have an orientation opposite to motifs 1 and 2. The feature marked by a black circle is the start of growth of Pb at the next height. The inset shows a fast Fourier transform of the STM image, showing τ-scaled maxima. (c) and (d) Height histograms taken from (a) and (b). Labeled in (d) are the contributions from Pb atoms and the surface. (e) A composite of (c) and (d), comparing the distribution of the heights in (a) and (b).

both) is adsorbing directly on top of these atoms. Pb atoms at z values larger than height 4 are also observed, as shown by the small number of counts in Fig. 3(e). At much larger dose times ($\sim$180 min), these atoms begin to form periodic structures.

To compare the overall system of Pb heights, Fig. 3(f) shows a composite of the histograms from Figs. 2(d), 3(d), and 3(e). Each histogram is colored as before, with a key

TABLE I. The heights and edge lengths of motifs of Pb observed in Figs. 3(b)–3(d), compared to their model plane counterparts in Figs. 4(b)–4(d). Heights are measured with respect to the surface.

Height	Height$_{STM}$ (nm)	Height$_{model}$ (nm)
1	0.06 ± 0.01	0.053
2	0.11 ± 0.01	0.110
3	0.23 ± 0.01	0.231
4	0.35 ± 0.02	0.346
Motif	Edge$_{STM}$ (nm)	Edge$_{model}$ (nm)
1	2.6 ± 0.1	2.54
2	1.5 ± 0.1	1.42
3	0.91 ± 0.05	1.04
4(S)	1.47 ± 0.05	1.57
4(L)	2.4 ± 0.1	2.54
5	1.62 ± 0.07	1.57

showing which heights are represented by each chart (S = substrate). Here, the substrate shoulder from the low-coverage data has been used as an initial calibration point for comparing Fig. 3(d), highlighted with a dashed line at 0 nm. Subsequently, the first height is used as a reference point. The overlap of height 2 in Figs. 3(d) and 3(e) is shown by the second dashed line, at $\sim$0.11 nm. The comparison of the histograms shows the extent to which the overall height distribution is broadened by the additional Pb atoms. Likewise, the defined peaks of the third and fourth heights infer that the Pb produces a network of isolated structures on top of the first layer.

IV. DISCUSSION

A. Adsorption sites of each layer

The distinctive heights of the Pb atoms above the substrate can be recognized from the histograms. Following the methodology in [17], we can compare these values to the heights of planes above the surface in the Cd-Yb model. If a model plane with a similar height for each set of Pb is found, we then compare motifs from these planes to the features formed by the Pb atoms. If a "match" is found, we attribute the adsorption sites of each height to positions explained by these planes. Figure 4(a) shows the heights and densities of the model planes above the surface, color-coded to represent and match the shells of the Cd-Yb clusters (Fig. 1) which form
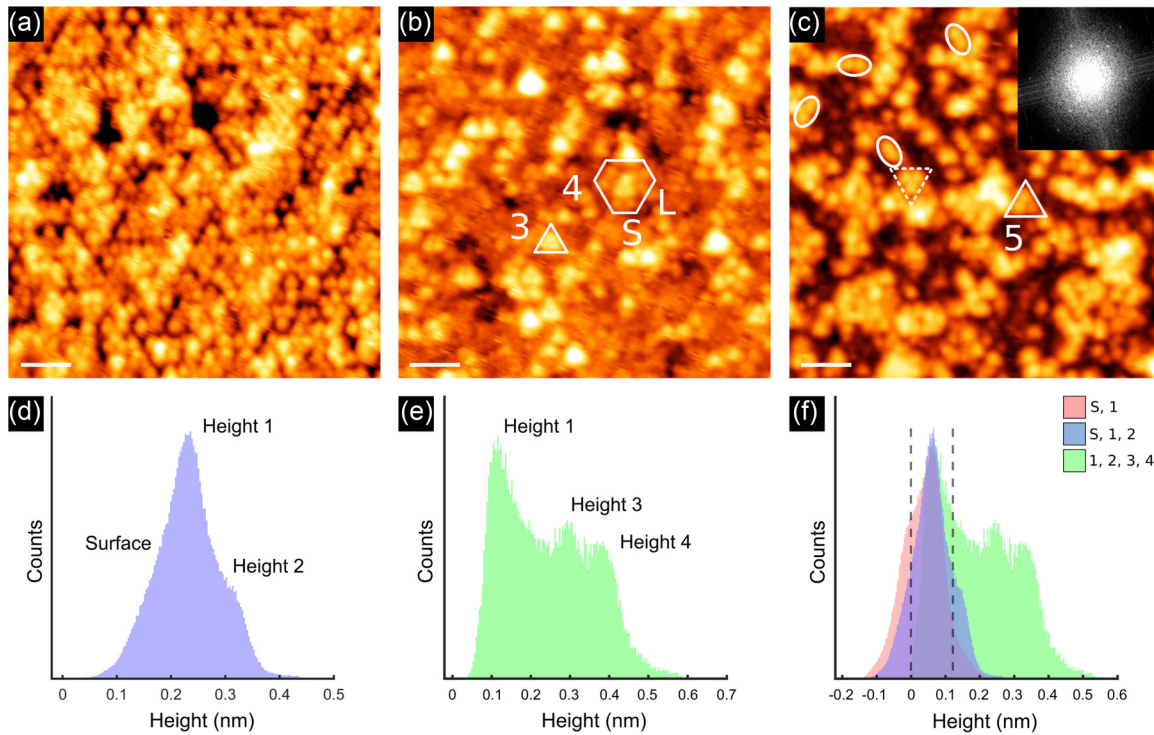
FIG. 3. (a) STM image of the surface after Pb dosing for 15 min. The scale bar is 6 nm. (b) STM image of the surface after Pb dosing for 30 min. Marked in white are a triangle labeled 3 and a distorted hexagon (4), with edge lengths S and L, listed in Table I. The scale bar is 6 nm. (c) STM image of the surface after Pb dosing for 120 min. Motif 5 is marked by a white triangle; the dashed triangle shown has opposite orientation. Pb dimers with the same edge length as motif 5 are also marked by ovals. The inset shows a τ-scaled FFT, taken considering only height 4 atoms. The scale bar is 4 nm. (d) and (e) Histograms from (a) and (c). (f) A composite of histograms from (d) and (e) and Fig. 2(d).

each plane. Each height is marked, with the corresponding model shell also labeled.

Pb atoms at height 1 can be explained by a plane consisting of atoms from the fifth shells (red) of surface-centered clusters. Its morphology is shown in Fig. 4(b), where collections of closely separated Pb atoms form triangular motifs. These dense groups may be the cause of the enlarged protrusions observed in Fig. 2(b). Motifs with edge lengths equal to those measured in Fig. 2(b) are highlighted, and motif 1 has been enlarged and compared to the data in Fig. 4(e).

The adsorption positions of height 2 Pb atoms are difficult to analyze independently, as these atoms are covered by height 3 atoms quickly. However, we can resolve the third height, then use limited examples of comparative geometry between the second and third heights to find the plane which explains the height 2 Pb atoms. Height 3 Pb atoms largely form only one motif, a small triangle with only one orientation (motif 3). Combining the height of the atoms with this observation leads to the assignment of a plane of fourth-shell (blue) atoms originating from surface-centered clusters, shown in Fig. 4(c). Now, motif 4, shown in Fig. 4(f), is a motif 3 triangle surrounded by six atoms at height 2 which create a distorted hexagon. This particular triangle-in-hexagon formation is only observed by STM between these two heights, and likewise, only one plane can be used to explain the positions of the height 2 atoms in this structure. Labeled in Fig. 4(a), this height is explained by the third shell (green, Yb) of surface-centered clusters. Figure 4(c) shows the superposition of heights 2 and 3 at this formation. The adsorption sites of

the final Pb atoms can be explained by third-shell (green, Yb) positions of off-surface-centered clusters, labeled in Fig. 4(a) and shown in Fig. 4(d). As with heights 2 and 3, examples of comparative geometry between heights 3 and 4 which match those seen in the model can be found. In Table I, we collect all of the experimental motif edge lengths and their counterparts identified in the model for comparison.

B. Stability of quasicrystalline Pb

Pb adsorption sites on the threefold i-Ag-In-Yb surface can be explained by "vacant" i-Cd-Yb planes in the same way as was found for the fivefold surface. However, the actual growth mode differs here—rather than a layer-by-layer type, Pb favors growth directly perpendicular to the surface. One explanation is that this is due to the relative change in density of available adsorption sites between these two surfaces.

The major difference (aside from rotational symmetry) between the three- and fivefold orientations of i-Ag-In-Yb is atomic density within planes perpendicular to these directions. The average number of atoms per plane for the threefold direction is 2.6 atoms/nm^2, and that for the fivefold direction is 4.6 atoms/nm^2. Likewise, the density of planes in a 1-nm slab in z is 54 planes/nm for the threefold direction and 38 planes/nm for the fivefold direction. In other words, the threefold orientation has fewer atoms per plane, but more planes per nanometer in z compared to the fivefold orientation. The implication is that there are a reduced number of available adsorption sites in the threefold x-y plane compared to the
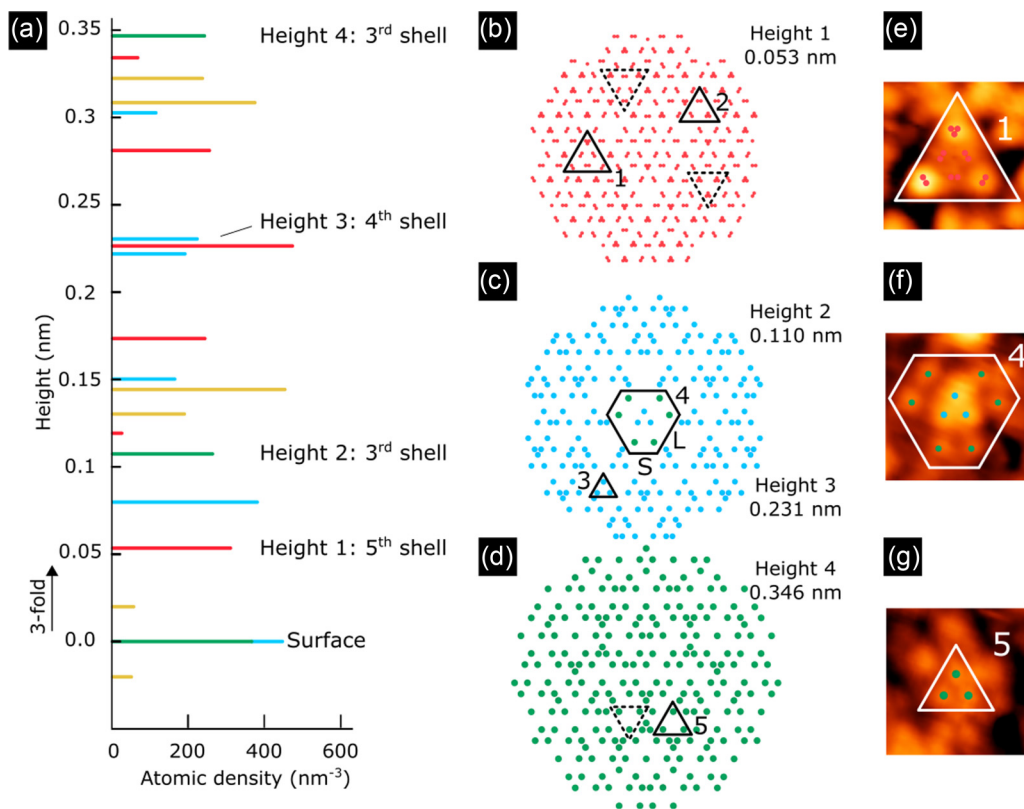
FIG. 4. (a) Distribution of the height and density of atoms of i-Cd-Yb along the threefold direction. Labeled are shells of the bulk clusters which correspond to the observed Pb heights as indicated. The surface plane is also indicated. The color scheme is the same as in Fig. 1. (b)–(d) In-plane atomic structure at indicated heights. Marked in each panel are similar motifs from Figs. 2(b), 3(b) and 3(c). The heights of the planes are shown above each. Only selected atoms at height 2 are shown for clarity in comparison with STM. (e)–(g) Selected STM motifs from heights in (b)–(d), respectively.

fivefold direction. Therefore, once these sites are filled, Pb will occupy preferential sites available in the z direction.

This observation is strengthened when analyzing the nearest-neighbor distances between Pb atoms within this growth scheme. The stability and growth mode of Pb on the fivefold i-Ag-In-Yb surface was stabilized by the reduction of nearest-neighbor distances [17]. In this case, values close to or less than the nearest-neighbor value in crystalline (fcc) Pb (0.32 nm) were considered to be important in stabilizing the film, verified by density functional theory calculations. Employing a similar argument here, Table II shows the nearest-neighbor values taken from the threefold planes in Figs. 4(b)–4(d) for intraplane (i.e., separations of atoms belonging to the same plane) and interplane (separations between different planes) distances. Here, (S–1) refers to the distance measured between a substrate atom and a height 1 atom, etc.

In the intraplane case, two distances are measured for each model plane, as the nearest-neighbor distance can vary on an atom-by-atom basis. The average value for each plane shows that intraplane nearest-neighbor distances are much larger than the bond length for crystalline Pb. However, the values for the interplane distances are identical or close to the nearest-neighbor distance for crystalline Pb (with the exception of heights 2–3). Thus, we hypothesize that to maximize the film's stability, positions in z are prioritized over in-plane growth and, in particular, the height 1 atoms are important for stabilizing the larger-height atoms (3 and 4).

To illustrate this argument, Fig. 5 shows a truncated Tsai-type cluster which is decorated with colored atoms. This schematic shows how a single Tsai cluster can be "capped"

TABLE II. Top: Intralayer distances of the model planes. NN_i refers to distances which are observed with equal regularity. The asterisked value shows a nearest-neighbor distance close to crystalline Pb. Bottom: Interlayer distances which are close to crystalline Pb.

Height	Intraplane distance (nm)		
	NN_1	NN_2	Average
1	0.30*	0.97	0.63
2	0.60	0.97	0.78
3	0.52	1.04	0.78
4	0.60	0.97	0.78
	Interplane distance (nm)		
	Height		NN
	S–1		0.32
	S–2		0.34
	1–2		0.34
	1–3		0.32
	1–4		0.34
	2–3		0.60
	3–4		0.32
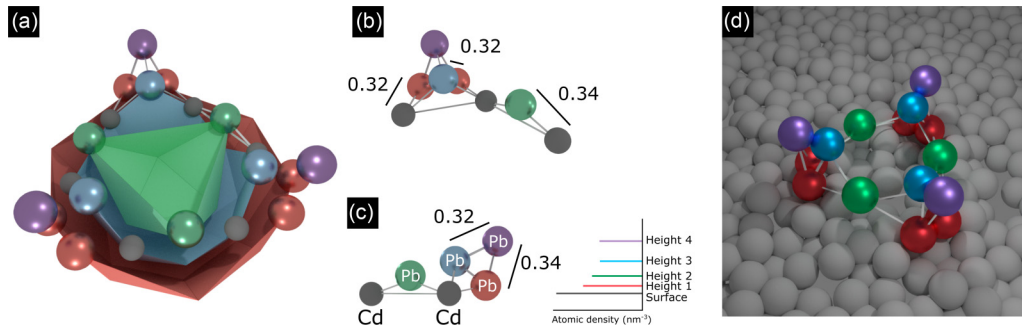
FIG. 5. (a) A Tsai cluster with the third, fourth, and fifth shells shown as truncated polyhedra. Each shell is decorated with Pb atoms, representing the planes which construct the film. (b) A section of (a) with nearest-neighbor values labeled in nanometers. (c) Side view of (b), with more nearest-neighbor values. Adjacent is a planar model with labeled planes for each height. (d) View of (a) on the threefold surface, from a different perspective.

by the four heights of Pb atoms. The colors of the truncated polyhedra and Pb atoms correspond to the similarly colored shells in Figs. 1 and 4(a). Surface atoms are colored gray, and height 4 atoms are colored purple to differentiate them from the height 2 atoms (both have positions modeled by third shells). The interplane nearest-neighbor distances are labeled in Figs. 5(b)–5(c), showing how the Pb atoms in the system are stabilized either by the substrate or previous heights, as opposed to atoms of the same height. Finally, Fig. 5(d) shows the Pb "cluster" of Fig. 5(a) from a different perspective on a model of the threefold surface (gray spheres). According to the Cd-Yb model, these Pb nanostructures would be distributed quasiperiodically over the surface.

V. CONCLUSIONS

We have shown that the growth scheme of Pb observed on the fivefold i-Ag-In-Yb surface also applies to the threefold surface. On this substrate, the low in-plane density of the threefold surface and the subsequent Pb layers creates a quasicrystalline network with isolated structures forming along z. Here, we have showcased the usage of a stable, sparse, and uniquely structured quasicrystalline surface which could potentially be used to produce templated nanostructures. The low density of the substrate provides a unique arena for this growth mode—similar atomic sparsity could be found only in a periodic system in a vicinal plane, in which case, the surface becomes unstable and facets. It would be interesting to investigate if adsorption of a stoichiometric blend of elements (e.g., Ag/In/Yb) that constitute the quasicrystal on this surface would indirectly replicate the building block Tsai-type clusters, providing direct evidence of the stability of bulk clusters.

[1] D. Shechtman, I. Blech, D. Gratias, and J. W. Cahn, Phys. Rev. Lett. **53**, 1951 (1984).

[2] R. Penrose, Math. Intell. **2**, 32 (1979).

[3] H. R. Sharma, M. Shimoda, and A. P. Tsai, Adv. Phys. **56**, 403 (2007).

[4] R. McGrath, J. Ledieu, E. J. Cox, and R. D. Diehl, J. Phys.: Condens. Matter **14**, R119 (2002).

[5] R. McGrath, J. A. Smerdon, H. R. Sharma, W. Theis, and J. Ledieu, J. Phys.: Condens. Matter **22**, 084022 (2010).

[6] R. McGrath, H. R. Sharma, J. A. Smerdon, and J. Ledieu, Philos. Trans. R. Soc. A **370**, 2930 (2012).

[7] S. Coates, J. A. Smerdon, R. McGrath, and H. R. Sharma, Nat. Commun. **9**, 3435 (2018).

[8] H. R. Sharma, J. A. Smerdon, P. J. Nugent, A. Ribeiro, I. McLeod, V. R. Dhanak, M. Shimoda, A. P. Tsai, and R. McGrath, J. Chem. Phys. **140**, 174710 (2014).

[9] V. Fournée, É. Gaudry, J. Ledieu, M.-C. De Weerd, D. Wu, and T. Lograsso, ACS Nano. **8**, 3646 (2014).

[10] J. A. Smerdon, J. Ledieu, J. T. Hoeft, D. E. Reid, L. H. Wearing, R. D. Diehl, T. A. Lograsso, A. R. Ross, and R. McGrath, Philos. Mag. **86**, 841 (2006).

[11] J. A. Smerdon, J. Ledieu, R. McGrath, T. C. Q. Noakes, P. Bailey, M. Draxler, C. F. McConville, T. A. Lograsso, and A. R. Ross, Phys. Rev. B **74**, 035429 (2006).

[12] J. A. Smerdon, L. Leung, J. K. Parle, C. J. Jenks, R. McGrath, V. Fournée, and J. Ledieu, Surf. Sci. **602**, 2496 (2008).

[13] J. A. Smerdon, J. K. Parle, L. H. Wearing, T. A. Lograsso, A. R. Ross, and R. McGrath, Phys. Rev. B **78**, 075407 (2008).

[14] J. A. Smerdon, K. M. Young, M. Lowe, S. S. Hars, T. P. Yadav, D. Hesp, V. R. Dhanak, A. P. Tsai, H. R. Sharma, and R. McGrath, Nano Lett. **14**, 1184 (2014).

[15] K. J. Franke, H. R. Sharma, W. Theis, P. Gille, P. Ebert, and K. H. Rieder, Phys. Rev. Lett. **89**, 156104 (2002).

[16] H. Takakura, C. P. Gómez, A. Yamamoto, M. de Boissieu, and A. P. Tsai, Nat. Mater. **6**, 58 (2007).

[17] H. R. Sharma, K. Nozawa, J. A. Smerdon, P. J. Nugent, I. McLeod, V. R. Dhanak, M. Shimoda, Y. Ishii, A. P. Tsai, and R. McGrath, Nat. Commun. **4**, 2715 (2013).

[18] S. S. Hars, H. R. Sharma, J. A. Smerdon, S. Coates, K. Nozawa, A. P. Tsai, and R. McGrath, Surf. Sci. **678**, 222 (2018).

[19] C. Cui, P. J. Nugent, M. Shimoda, J. Ledieu, V. Fournée, A. P. Tsai, R. McGrath, and H. R. Sharma, J. Phys.: Condens. Matter **24**, 445011 (2012).